CSIRO PUBLISHING
www.publish.csiro.au/journals/ajb *Australian Journal of Botany*, 2009, **57**, 512–523

Phytolith analysis of Cyperaceae from the Pampean region, Argentina

Mariana Fernández Honaine[A,C,D], *Alejandro F. Zucol*[B,C] *and Margarita L. Osterrieth*[A]

[A]Instituto de Geología de Costas y del Cuaternario, Facultad de Ciencias Exactas y Naturales, Universidad Nacional de Mar del Plata, CC 722, Correo Central, (7600) Mar del Plata, Buenos Aires, Argentina.
[B]Laboratorio de Paleobotánica, Centro de Investigaciones Científicas (CICYTTP–CONICET), Dr Materi y España (E3105BWA) Diamante, Entre Ríos, Argentina.
[C]Comisión Nacional de Investigaciones Científicas y Tecnológicas (CONICET).
[D]Corresponding author. Email: fhonaine@mdp.edu.ar

Abstract. Cyperaceae, along with Poaceae, is the main silica accumulator. Although the anatomical-taxonomic and palaeobotanical relevance of phytoliths has been well established, there are no studies that deal with the qualitative and quantitative aspects of the phytolith production or differentiate phytoliths from the different organs in Cyperaceae. Toward the construction of a detailed database of phytolith production, we describe in the present paper the phytoliths of leaves, culms and fruits of Cyperaceae from Pampean region (Argentina). Phytoliths were extracted by a calcination technique. Qualitative and quantitative characters and percentages of phytolith morphotypes were subject to principal component analysis to analyse their taxonomic relevance. For some sedges, values of phytolith content and a comparative analysis of leaves, culms and fruit phytoliths are presented here for the first time. Diverse tissues such as epidermis, xylem, parenchyma and sclerenchyma produced phytoliths. The most abundant morphotypes were conical phytoliths, which showed differences in the base shape and in their size between organs. Leaf/culm cones have a rounded, rectangular or square base; typical fruit cones have a polygonal base and they are bigger and more robust. PCA showed that quantitative and qualitative characters of cones, along with the percentages of morphotypes, allowed group distinction.

Introduction

Cyperaceae is one of the main silica accumulators, along with Poaceae family (Piperno 1988; Ollendorf 1992). Duval-Jouve (1873) and Wilczek (1892) were the first researchers who described the 'cone-shaped' silica bodies in epidermal cells overlying the sclerenchyma, in leaves, culms and fruits of Cyperaceae. Mehra and Sharma (1965) not only described the silica bodies in several species but also explained their development in *Eriophorum comosum* Wall. ex Nees. Later, Metcalfe (1971), in his anatomical study of Cyperaceae, described and classified the different silica body shapes of leaves and culms. Since then, many other anatomic studies of these silica bodies have been conducted (Schuyler 1971; Gordon-Gray *et al*. 1978; Ragonese *et al*. 1984; Bruhl *et al.* 1992; Browning and Gordon-Gray 1995; Bruhl 1995).

Phytoliths (and particularly the silicophytoliths or silica bodies) are widely used as microfossil indicators of past plant communities, as well as indicators of environmental conditions where these communities developed (Rovner 1971; Alexandre *et al.* 1997; Barboni *et al*. 1999). The typical phytoliths of Cyperaceae are conical morphotypes that can be easily distinguished from the phytoliths produced by other families (Ollendorf 1992). This morphological differentiation allows the identification of sedge communities in fossil record. Although sedge phytoliths are underrepresented relative to grasses in fossil record, various studies identified members of Cyperaceae family in soils and sediment sequences (Bonomo *et al.* 2009; Iriarte and Paz 2009). Also, sedge phytoliths can indicate specific palaeoenvironmental conditions, because many sedges grow in marshy or aquatic habitats or pseudogley–hydromorphic soils (Borba-Roschel *et al.* 2006; Iriarte 2006). Some sedges have been used for human activities, and phytolith analysis represents a valuable tool for identification of these plants in archaeological contexts (Chevalier 2008). Finally, silica bodies have been applied to taxonomic studies in the Cyperaceae family (e.g. Toivonen and Timonen 1976; Browning and Gordon-Gray 1995).

Despite the well established palaeobotanical, archaeological and anatomical-taxonomic relevance of sedge phytoliths, few studies have described or classified them as isolated particles, except for Ollendorf (1992), who developed the first schema for their classification. Furthermore, no studies have specifically analysed the qualitative and quantitative aspects of the phytolith production or clearly distinguished phytoliths from different organs of these plants. This kind of information is essential for adequate palaeobotanical, palaeoenvironmental and/or archaeological interpretations (Blinnikov 2005; Borba-Roschel *et al.* 2006).

© CSIRO 2009 10.1071/BT09041 0067-1924/09/060512

To advance towards a construction of a detailed reference collection of phytoliths in Argentine sedges, we describe phytolith morphotypes in leaves, culms and fruits of the most common species from Pampean region. Because conical phytoliths are diagnostic of this family, quantitative and qualitative features are determined on them to analyse their taxonomic relevance within the family. The results also complement the phytolith analysis carried out on Poaceae species from this region (Fernández Honaine *et al.* 2006). Because most of the species selected represent genera with a wide distribution, data obtained can also be applied to and/or compared with those from species from different regions.

Materials and methods

Thirteen species, corresponding to the main sedges that characterise ponds and aquatic habitats from the Pampean region in Argentina, were selected (Table 1). The species were sampled at Instituto de Botánica Darwinion Herbarium (SI Herbarium, San Isidro, Buenos Aires, Argentina) and the Reserva Integral Laguna de los Padres, Buenos Aires Province, Argentina.

Leaves (or culms in *Eleocharis* spp. and *Schoenoplectus californicus*) and fruits from at least two specimens of each species were collected, and phytoliths were extracted following a calcination technique (Labouriau 1983). The samples were first placed in an ultrasound bath for 15–20 min and washed with distilled water to remove mineral contaminants. The material was dried at 56°C for 24 h, and charred at 200°C for 2 h. Later, it was boiled in a 5 N HCl solution for 10 min, washed with distilled water and filtered with ashless filter paper, until no more chloride ions were detected. Finally, the material was ignited at 760°C for 3 h. Silica content was calculated as a percentage dry weight.

The ashes were mounted with immersion oil and the phytolith morphotypes were observed and described with a Leitz Wetzlar D 35780 microscope (Ernest Leitz GMBH Wetzlar, Germany) at ×400 magnification and a scanning electron microscope (JEOL JSM-6460 LV, Japan) at Universidad Nacional de Mar del Plata, Argentina. Photographs were taken with a digital camara Kodak Easy Share CX7530 (Eastman Kodak, Rochester, NY, US). More than 200 phytoliths were counted in each slide and the morphotypes were described according to Ollendorf (1992) and the ICPN descriptors (Madella *et al.* 2005). In each slide, at least 30 cones were observed and the following characters were described and measured (Fig. 1): height and shape of the apex, shape of the base, length of the smallest and longest axes, side number of the base (only in fruit cones), edge of the base (only in fruit cones). As a complement of phytolith description and with the purpose to localise the phytoliths in the tissue, leaves were hand-sectioned transversely and, in some cases, stained with phenol.

Principal component analyses (PCA) were carried out with the purpose of evaluating the relevance of the quantitative and qualitative characters of cone phytoliths and/or the phytolith morphotypes in the differentiation of the group analysed. The quantitative and qualitative characters were measured on leaf/culm cone phytoliths (1, apex height; 2, base shape; 3, length of the longest axis of the base; 4, length of the smallest axis of the base) and on fruit cone phytoliths (5, apex height; 6, apex shape; 7, length of the longest axis of the base; 8, length of the smallest axis of the base; 9, side number of the base; 10, edge of the base). The values for the continuous quantitative variables (1, 3, 4, 5, 7 and 8) were calculated as the mean value of all the measurements for each species; in discrete quantitative variables (9), the mode was calculated. Qualitative variables (2, 6 and 10) were codified. PCA was carried on the basis of a correlation matrix of the data.

Results

Silica content

The silica content ranged between 1.3 and 12.8% in the leaves, 1.6 and 11.4% in the culms, and 0.96 and 18.3% in the fruits (Fig. 2). The mean values in the leaves were similar for *Carex* spp. and *Rhynchospora* spp. (5.6–6.6%), whereas *Cyperus* had the greatest variability (2.9–7.8%). With respect to culm silica contents, *Eleocharis bonariensis* had the greatest mean value (9.55%), which was also higher than the values for the leaves from the other taxa. In fruit analyses, the silica content showed more variability within genera than did that for the leaves; the highest mean was found in *Cyperus reflexus* (9.39%), whereas the smallest was found in *Schoenoplectus californicus* (1.14%) (Fig. 2).

Phytolith description

Carex

In the three studied species, articulated and isolated cones ('typical leaf cones') were the dominant morphotype in the leaf phytolith assemblage (62.6% in *C. phalaroides*, 48.1% in *C. chilensis* and 47.7% in *C. tweediana*) (Fig. 3*a*, Table 2). Cones had a variable basal shape and, along with the cones of *Rhynchospora*, were the biggest in the group analysed (Table 3). Other abundant morphotypes were elongate psilate phytoliths (24.4% in *C. chilensis*, 16% in *C. tweediana*, 12% in *C. phalaroides*), silicifications of cell walls (13.4% in *C. chilensis*), silica skeletons composed of cones and elongate psilate phytoliths (13.8% in *C. phalaroides*, 8.1% in *C. tweediana*) and silica skeletons composed of diverse silicified cells, such as cones, xylem elements and elongate phytoliths (16% in *C. tweediana*) (Fig. 3*v*, *w*).

The most abundant morphotypes in the fruit phytolith assemblage were cones with polygonal bases (polygonal cones) (78.8% in *C. chilensis*, 69.3% in *C. tweediana* and 55.5% in *C. phalaroides*) (Fig. 4*a–d*, Table 2). Together with the typical leaf cones, the polygonal cones are, along with the cones of *Rhynchospora*, the biggest in the group analysed. Within *Carex* species, the biggest polygonal cones were produced by *C. tweediana* (Table 3). In *C. phalaroides*, the typical leaf cones were also abundant (39.7%). *C. tweediana* assemblage was also characterised by cylindrical dendriform phytoliths, which were found articulated (5.6%) or isolated (8.7%) (Fig. 4*p*).

Cyperus

Articulated or isolated typical leaf cones were the dominant morphotype in the leaf phytolith assemblage in the five species analysed (93.8% in *C. odoratus*, 80.5% in *C. reflexus*, 69.6% in *C. corymbosus*, 47% in *C. digitatus* and 42.1% in *C. eragrostis*) (Fig. 3*b–d*, Table 2). In some cases, these morphotypes were also

Table 1. Sedge species selected for the study

Species	Abbrev.	Collector and code herbarium	Location and date of collection	No. of specimens collected for leaf/culm analysis	No. of specimens collected for fruit analysis
Carex chilensis Brongn	Cac	Fernández Honaine 17 (Laboratorio de Geoecología de suelos, FCEyN, UNMdP)	Buenos Aires, Laguna de los Padres, 27 Dec. 2000	4	2
C. phalaroides Kunth	Cap	Guaglianone *et al.* 3090 (SI)	Buenos Aires, I. Martín García, 25 Oct. 1996	3	3
		Lafranchi 735 (SI)	Buenos Aires, Tigre, 29 Sep. 1948		
		Burkart 18 441 (SI)	Buenos Aires, Pehuajó, 14 Oct. 1950		
C. tweediana Nees	Cat	Guaglianone *et al.* 3103 (SI)	Buenos Aires, I. Martín García, 25 Oct. 1998	3	3
		Hurell *et al.* 1568 (SI)	Buenos Aires, I. Martín García, 9 Dec. 1993		
		Burkart 9263 (SI)	Buenos Aires, Delta Paraná, 28 Nov. 1938		
Cyperus corymbosus var. *subnodosus* Rottböll	Cyc	Burkart 12 839 (SI)	Buenos Aires, Ramallo, 28 Dec. 1941	3	3
		Guaglianone and Santoro 243 (SI)	Buenos Aires, 9 de Julio, 28 Feb. 1979		
		Burkart 6681 (SI)	Buenos Aires, Zelaya, 23 Dec. 1934		
C. digitatus Roxburgh	Cyd	Koyama 13 666 (SI)	Buenos Aires, Tigre, 18 Feb. 1970	3	3
		Guaglianone and Santoro 237 (SI)	Buenos Aires, 9 de Julio, 28 Feb. 1979		
		Rodriguez 123 (SI)	Buenos Aires, Quilmes, 14 Dec. 1912		
C. eragrostis Lam.	Cye	C.M.Hicken SI 1698	Buenos Aires, Mar del Plata, 5 Jan. 1933	5	5
		C.M.Hicken SI 1685	Buenos Aires, Mar del Plata, 5 Jan. 1933		
		A.E.Lanfranchi 936 (SI)	Buenos Aire, Tigre, 3 Dec. 1951		
		Alvarez *et al.* 250 (Laboratorio de Geoecología de suelos, FCEyN, UNMdP)	Buenos Aires, Canteras Batán, 2 Mar. 2005		
		Fernández Honaine *et al.* 245 (Laboratorio de Geoecología de suelos, FCEyN, UNMdP)	Buenos Aires, Canteras Batán, Dec. 2006		
C. odoratus L.	Cyo	Hurrell *et al.* 6155 (SI)	Buenos Aires, Berisso, 25 Mar. 2006	3	3
		Lanfranchi 1806 (SI)	Buenos Aires, Tigre, 17 Mar. 1971		
		Lanfranchi 1725 (SI)	Buenos Aires, Laguna de los Padres, 19 Feb. 1970		
C. reflexus Vahl	Cyr	Barros 2271 (SI)	Buenos Aires, Mar del Plata, 12 Feb. 1931	3	3
		Pesce 46 (SI)	Buenos Aires, Rojas, Jan. 1942		
		Alvarez *et al.* 243 (Laboratorio de Geoecología de suelos, FCEyN, UNMdP)	Buenos Aires, Canteras Batán, Dec. 2006		
Eleocharis bonariensis Nees	Elb	Lanfranchi 40 (SI)	Buenos Aires, Tigre, 31 Oct. 1943	4	3
		Burkart 10 027 (SI)	Buenos Aires, Lobos, 23 Dec. 1939		
		Hicken 104 (SI)	Buenos Aires, Mar del Plata, 15 Nov. 1930		
		Alvarez *et al.* 249 (Laboratorio de Geoecología de suelos, FCEyN, UNMdP)	Buenos Aires, Canteras Batán, 2 Mar. 2005		
E. macrostachya Britton (Elm)	Elm	Burkart 17510 (SI)	Buenos Aires, Jáuregui, 20 Nov. 1948	3	3
		Cabrera 8520 (SI)	Buenos Aires, Pdo. Gral Lavalle, 1 Dec. 1944		
		Barros 176 (SI)	Buenos Aires, Capital Federal, 15 Nov. 1925		

Table 1. (*continued*)

Species	Abbrev.	Collector and code herbarium	Location and date of collection	No. of specimens collected for leaf/culm analysis	No. of specimens collected for fruit analysis
Pycreus tener C.B. Clarke ex Chodat et Hassl.	Pyt	Pedersen 13369 (SI)	Corrientes, Depto. Concepción, 10 Mar. 1982	2	2
		Barros 242 (SI)	Buenos Aires, Vicente López, 25 Dec. 1925		
Rhynchospora corymbosa var. *bonariensis* Barros ex Cabrera and G. Dawson	Rhc	Hurrell *et al.* 6305 (SI)	Buenos Aires, Archipiélago Solís, 16 Dec. 2006	3	3
		Guaglianone and Dopchiz 2811 (SI)	Buenos Aires, San Isidro, 1 Nov. 1995		
		Ragonese and Guaglianone SI 26 178	Buenos Aires, Punta Lara		
Schoenoplectus californicus (C.A.Mey.) Soják	Scc	Fernández Honaine 26 (Laboratorio de Geoecología de suelos, FCEyN, UNMdP)	Buenos Aires, Laguna de los Padres, 27 Dec. 2000	3	2

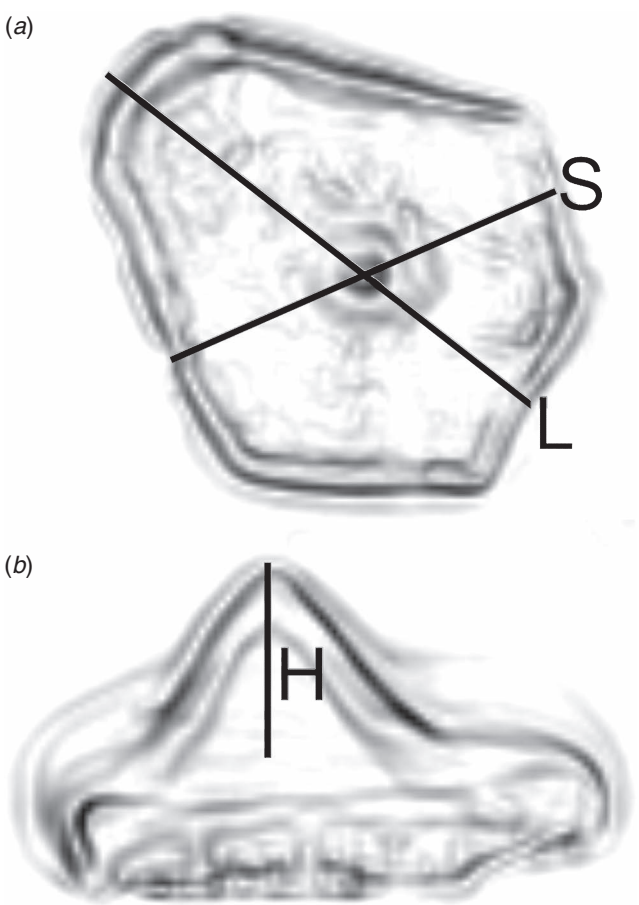

Fig. 1. Schematic representation of some characters measured on conical phytoliths. (*a*) Surface view; (*b*) side view. S, shortest axis; L, longest axis; and H, height of the apex.

articulated with elongate psilate phytoliths (20% in *C. eragrostis*, 11.4% in *C. corymbosus*, 7.1% in *C. digitatus* and 5.6% in *C. reflexus*) (Fig. 3*i*). Cones had a rounded, rectangular or square base outline, and a pointed or truncated apex; *C. eragrostis* and *C. reflexus* had the biggest cones (Table 3). Elongate psilate phytoliths (*C. corymbosus*, *C. digitatus* and *C. eragrostis*), silica skeletons composed by diverse silicified cells (*C. digitatus* and *C. eragrostis*) and isolated parallelepipedal psilate phytoliths (*C. digitatus*; Fig. 3*u*) were also very abundant in some leaf assemblages of *Cyperus*.

In fruit phytolith assemblage, polygonal cones (87.8% in *C. reflexus*, 77.3% in *C. eragrostis*, 76.5% in *C. odoratus*, 42.1% in *C. digitatus* and 40.9% in *C. corymbosus*) and the typical leaf cones (56.8% in *C. corymbosus*, 52.8% in *C. digitatus*, 22.3% in *C. odoratus*, 20.7% in *C. eragrostis* and 12% in *C. reflexus*) were the dominant morphotypes (Fig. 4*e–l*, Table 2). An important variation in the apex shape and in the edge of the polygonal cones was observed among species. The cones of *C. digitatus* had very sinuate edges and a rugose surface, with some having no apex, and others having multiple apices. *C. reflexus* was characterised by cones with sinuate perforated edges, multiple apices or without an apex. *C. odoratus* and *C. eragrostis* had the largest cones, with lightly sinuate edges. *C. corymbosus* had psilate-edge cones, with some not having an apex (Table 3).

Eleocharis

Articulated and isolated typical leaf cones (65.2% in *E. bonariensis* and 87.8% in *E. macrostachya*) were the most abundant morphotype in culm assemblages (Fig. 3*e*, Table 2). The base of these cones was of variable shape, and they were the smallest in the group analysed (Table 3). Silica skeletons composed by silicified cell walls (19.5% in *E. bonariensis* and 5.4% in *E. macrostachya*) and isolated parallelepipedal psilate phytoliths (5.6% in *E. bonariensis*) were also abundant in the culm assemblages of *Eleocharis*.

Polygonal cones were not found in the fruits of these species. Instead, silica skeletons composed of rectangle sinuate or psilate cells arranged in parallel rows (51.3% in *E. bonariensis* and 43.9% in *E. macrostachya*) were the most abundant morphotype (Fig. 4*r*, Table 2). These morphotypes corresponded to silicification of the lumen and/or the walls of

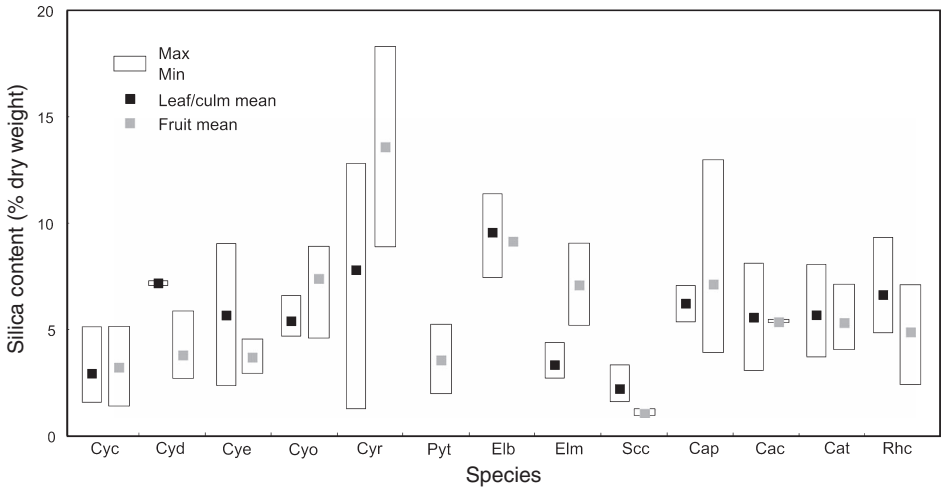

Fig. 2. Dry weight percentage of silica content of leaves, culms and fruits of Cyperaceae species. Abbreviations are as given in Table 1.

the cells. Cones similar to those produced in culms (37% in *E. bonariensis* and 32.7% in *E. macrostachya*) were also very common in the assemblages.

Pycreus tener

Articulated and isolated cones (69.1 and 18.7%, respectively) dominated leaf phytolith assemblage (Fig. 3*f*, *j*, Table 2). These morphotypes had a rounded, rectangular or square base and a pointed apex of 5-µm height (Table 3). Articulated and isolated elongate psilate phytoliths (2.5 and 2.3%, respectively), silica skeletons composed of cones and elongate psilate (2.3%) and elongate sinuate phytoliths (1.9%) were also observed.

Fruit phytolith assemblage was characterised by articulated (51.3%) and isolated (29.8%) polygonal cones (Fig. 4*m*, Table 2). Cones similar to those found in leaves were also common in fruit assemblages (18.4%).

Rhynchospora corymbosa

The most abundant morphotypes in the leaf phytolith assemblage were articulated or isolated stellate phytoliths (36.5%) (silicifications of stellate cells derived from aerenchyma) and cones (25.4%) (Fig. 3*g*, *q*, *r*, Table 2). Cones, which were the biggest in the group of sedges analysed, were also found articulated with elongate psilate phytoliths. Silica skeletons composed of multiple cell types (13.1%), articulated and isolated elongate psilate phytoliths (12.1%) and stomatal complexes (7.5%) were also abundant.

Articulated (43.3%) and isolated (22.4%) polygonal cones with smooth edges were dominant in the fruit phytolith assemblage (Fig. 4*n*, *o*, Tables 2, 3). These polygonal cones were the biggest in the group analysed in the present paper. Typical leaf cones (13.5%), cylindrical dendriform phytoliths (9.8%) (Fig. 4*q*) and elongate sinuate phytoliths (6.5%) were also observed.

Schoenoplectus californicus

Culm phytolith assemblage was mainly characterised by articulated and isolated typical leaf cones (43.1 and 13.4%, respectively) (Fig. 3*h*), and silica skeletons composed by cones, rectangular and parallelepipedal cells and xylem elements (37.6%) (Table 2). Other morphotypes observed were articulated or isolated parallelepipedal psilate phytoliths (3.2%), articulated or isolated rectangular psilate phytoliths (0.9%), cylindrical sulcate tracheid (0.1%) and stomatal complexes (0.6%). The typical leaf cones had a variable basal shape and were the smallest in the sedge group analysed (Table 3).

Articulated and isolated cones (62%), such as those found in culm assemblages, and articulated and isolated rectangular psilate phytoliths (21%) were the most abundant morphotype in fruit assemblages. Polygonal cones (with psilate edges and 5–7 basal sides) had a low degree of silicification and they were present in small numbers (5.6%) (Fig. 4*s*). Other observed morphotypes were cylindrical sulcate tracheid (5.6%), silica skeletons (2.9%), and parallelepipedal psilate phytoliths (1.5%).

Silica bodies observed in transverse sections of leaves and culms

Transverse sections of leaves or culms show that conical silica bodies are restricted to epidermal cells overlying sclerenchyma, as it was described previously (Duval-Jouve 1873; Wilczek 1892; Metcalfe 1971; Bruhl *et al*. 1992) (Fig. 3*k–p*). This association was reflected by the silicification process, where the silica skeletons composed of cones and elongate psilate phytoliths corresponded to epidermal cells + sclerenchyma fibers (Fig. 3*i*, *j*). Usually, these epidermal cells are smaller than the rest of the cells and show only one cone (in transverse section). In leaves, cones are mainly observed in abaxial epidermis, although they are present in both layers on epidermis at the edge of leaves in some species (e.g. *Cyperus eragrostis*, *Cyperus reflexus* and *Rhynchospora corymbosa*). Sections from stained leaves of *R. corymbosa* showed the aerenchyma cells silicified (stained with phenol), which originated the stellate phytoliths found in this species (Fig. 3*s*, *t*).

Principal component analyses

The first three axes of the PCA, where only the quantitative and qualitative characters of conical phytoliths were used, accounted for 88.041% of the total variance (62.361% for Axis 1, 13.575%

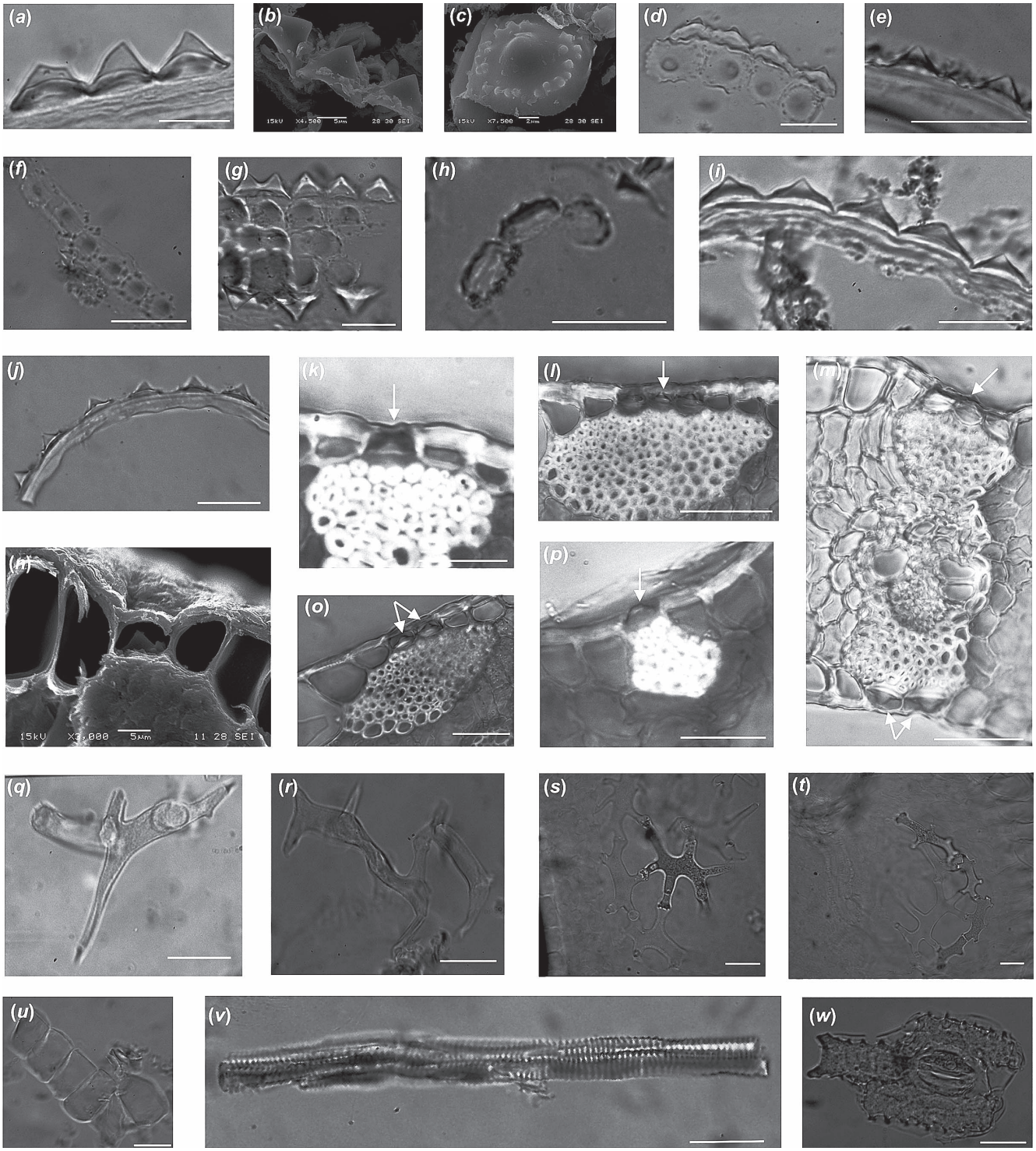

Fig. 3. Leaf/culm assemblages and anatomical sections. Conical phytoliths in (*a*) *Carex phalaroid*es, (*b*, *c*) *Cyperus odoratus*, (*d*) *Cyperus reflexus*, (*e*) *Eleocharis macrostachya*, (*f*) *Pycreus tener*, (*g*) *Rhynchospora corymbosa* and (*h*) *Schoenoplectus californicus*. Cones and elongate psilate phytoliths in (*i*) *Cyperus corymbosus* and (*j*) *Pycreus tener*. Transverse sections showing cone location (arrows) in (*k*) *Carex chilensis*, (*l*) *Cyperus eragrostis*, (*m*) *Carex phalaroides*, (*n*) *Schoenoplectus californicus*, (*o*) *Cyperus reflexus* and (*p*) *Eleocharis bonariensis*. (*q*, *r*) Stellate phytoliths in *R. corymbosa*. (*s*, *t*) Aerenchyma cells silicified (stained with phenol) in *R. corymbosa*. (*u*) Articulated parallelepipedal phytoliths in *C. digitatus*. (*v*) Cylindrical sulcate tracheid in *Carex chilensis*. (*w*) Stomatal complexes in *Carex tweediana*. Scale bar = 25 µm for all, except for *b*, *c* and *n* = 5 µm.

Table 2. Percentages of isolated and articulated phytolith morphotypes of sedge species

Abbreviations of species are as given in Table 1; L, leaf assemblage; C, culm assemblage; F, fruit assemblage. Values are means of at least two specimens

Morphotypes	Cac		Cap		Cat		Cyc		Cyd		Cye		Cyo		Cyr		Elb		Elm		Pyt		Rhc		Scc	
	L	F	L	F	L	F	L	F	L	F	L	F	L	F	L	F	C	F	C	F	L	F	L	F	C	F
Articulated																										
Leaf/culm cones	29.4	5.2	42.5	35.4	38.6	9.2	60.7	52	44	49.5	29.6	16.4	61.5	16.9	58.8	6.9	51.1	34.8	82.1	32.2	69.1	14.5	8.6	12.6	43.1	61.8
Polygonal cones	0	24.1	0	44.3	0	37.9	0	29.8	0	41.3	0	47.6	0	44.9	0	37.8	0	0	0	0	0	51.3	0	43.2	0	5.6
Elongate psilate	13.8	2.7	7.2	0.6	13.1	0	3.1	0	5.6	1.2	17.5	0	0.1	0	4.8	0	1.4	3.9	2.1	9.2	2.5	0.2	6.2	5.8	0.6	19.3
Elongate sinuate	0.6	0	0.8	1.2	1	0	0	0.2	0	0	0	0	0	0	0	0	0	0	0	0	0	0	0.4	0.1	0	0
Parallelepipedal psilate	1.8	0.2	0.8	0	0.7	0	1.6	0	2	0	0.3	0	1.1	0	0	0	0.5	0	0.3	0.3	0	0	0.4	0.3	0.6	1.5
Parallelepipedal sinuate	0	0	0	0	0.1	0	0	0	0	0	0	0	0	0	0	0	0	0	0	0	0	0	1.6	0	0	0
Cones + elongate psilate	2.8	0	13.8	0	8.1	2.3	11.4	0	7.1	1.7	20	0	0	0	5.6	0.1	0	0	0	0	2.3	0	12.2	0	0	0
Stomatal complexes	0	0	2.3	0	4.7	0	0.3	0	1.5	0	0.4	0	0.1	0	0.8	0	0.1	0	0.2	0.2	0	0	7.5	0	0.6	0
Cylindrical sulcate tracheid	0.3	3.8	0.5	0.3	1.3	0.9	1.2	1.1	4.1	1.1	1.2	1.7	0.1	0	0.8	0	0.4	0	0	4.7	0.4	0	0.1	1.3	0.1	5.6
Silicified walls	13.4	0	0.6	0	2.6	0	0	0	0	0	2.1	0	0	0	0	0	19.5	0	5.4	43.9	0	0	0	0	0	0
Silica skeletons	6.7	4.8	3.8	0.6	16	0	1.4	0.6	15.3	0.8	6.8	0	1.6	1.1	3	0	3.6	2.2	1.8	4.9	1.3	0.2	13.1	1.2	37.6	3.5
Silica skeletons (elongate arranged in parallel rows)	0	0	0	0	0	0	0	0	0	0	0	0	0	0	0	0	0	53.3	0	0	0	0	0	0	0	0
Prickles/hooks	1	0	0	0	0.9	2.3	0	0	0.2	0	0	0	0	0	0	0	0	0	0	0	0	0	0	1.5	0	0
Cylindrical dendriform	0	0.2	0	0	0	5.6	0	0	0	0	0	0	0	0	0	0	0	0	0	0	0	0	0	6.9	0	0
Stellate	0	0	0	0	0	0	0	0	0	0	0	0	0	0	0	0	0	0	0	0	0	0	5.8	0	0	0
Isolated																										
Leaf/culm cones	18.7	1	20.1	4.3	9.1	1.4	8.9	4.8	3	3.3	12.5	4.3	32.3	5.4	22.7	5.1	14.1	3.2	5.7	0.5	18.7	3.9	4.6	0.9	13.4	0.2
Polygonal cones	0	54.7	0	11.2	0	31.4	0	11.1	0	0.9	0	29.7	0	31.6	0	50	0	0	0	0	0	29.8	0	22.3	0	0
Elongate psilate	10.6	2.3	4.8	2	2.9	0.5	8.1	0.3	3.2	0.2	7.9	0.3	1.1	0.2	1.6	0	3.6	4.6	1.7	4.1	2.3	0	5.9	0.6	0.3	1.9
Elongate sinuate	0.3	0	2	0	0.6	0	1.1	0	0.5	0	0.3	0	0.7	0	0.2	0	0.1	1.2	0.2	0	1.9	0	0.1	0	0	0
Parallelepipedal psilate	0.7	0.4	0.3	0	0	0	2.3	0	13.4	0	1	0	0.3	0	0.8	0	5.6	0	0.6	0	1.5	0	0.4	0	2.7	0
Parallelepipedal sinuate	0	0	0	0	0	0	0	0	0	0	0.2	0	0	0	0.2	0	0.1	0	0	0	0	0	1	0	0	0
Prickles/hooks	0	0	0.5	0	0.1	0	0	0	0.2	0	0.1	0	0.9	0	0.9	0	0	0	0	0	0	0	0	0	0	0.6
Cylindrical dendriform	0	0.8	0	0	0	8.7	0	0	0	0	0	0	0	0	0	0	0	0	0	0	0	0	0	2.8	0	0
Stellate	0	0	0	0	0	0	0	0	0	0	0	0	0	0	0	0	0	0	0	0	0	0	30.7	0	0	0

Table 3. Qualitative and quantitative characters of leaf/culm and fruit cones

Species	Leaf or culm					Fruit						
		Base		Apex				Base			Apex	
	Shape	Smallest axis (μm)[A]	Largest axis (μm)[A]	Height (μm)[A]	Shape	Shape	Edges	No. of sides[B]	Smallest axis (μm)[A]	Largest axis (μm)[A]	Height (μm)[A]	Shape
Carex chilensis	Rectangular, rounded or square	7.5 (14) 22.5	7.5 (14.5) 25	5 (6.9) 10	Pointed or truncated	Polygonal	Smooth	5–8	10 (17.3) 37.5	25 (37.1) 55	7.5 (13.1) 17.5	Rounded
C. phalaroides	Rectangular or rounded	10 (14.8) 22.5	10 (19.6) 40	5 (7.5) 10	Pointed or truncated	Polygonal	Smooth	5–8	12.5 (21.7) 32.5	20 (29.4) 50	5	Rounded or NA
C. tweediana	Rectangular, rounded or square	7.5 (12.7) 17.5	10 (15.6) 25	5 (7.5) 7.5	Pointed	Polygonal	Smooth	5–8	12.5 (30.9) 50	25 (42.3) 65	7.5 (16.6) 25	Rounded or NA
Cyperus corymbosus	Rectangular or rounded	7.5 (12.6) 17.5	10 (14) 25	7.5	Pointed or truncated	Polygonal	Smooth	5–7	10 (15.1) 25	10 (20.3) 37.5	0 (1.8) 5	Truncated or NA
C. digitatus	Rectangular or rounded	10 (12.7) 17.5	10 (13.1) 27.5	5	Pointed or truncated	Rounded or polygonal	Very sinuate	4–6	7.5 (12.3) 15	10 (13.7) 22.5	5	Multiple apex
C. eragrostis	Rectangular, rounded or square	10 (14.9) 22.5	10 (19.4) 30	7.5 (7.5) 10	Pointed or truncated	Polygonal	Lightly sinuate	5–8	10 (20.3) 30	17.5 (30.6) 45	5 (5.5) 7.5	Rounded
C. odoratus	Rectangular or rounded	7.5 (12.7) 22.5	7.5 (13.1) 22.5	5 (5.1) 7.5	Pointed or truncated	Polygonal	Lightly sinuate	4–7	10 (19.3) 30	17.5 (27) 42.5	5	Truncated
C. reflexus	Rectangular, rounded or square	10 (15.5) 22.5	12.5 (17.8) 25	5 (7.4) 7.5	Pointed or truncated	Polygonal	Very sinuate, perforated	5–8	10 (14.9) 22	12.5 (19.4) 27	0 (5) 10	Multiple apex or NA
Eleocharis bonariensis	Rectangular or rounded	7.5 (10.5) 15	7.5 (11.4) 15	5 (5.6) 7.5	Pointed or truncated	–	–	–	–	–	–	–
E. macrostachya	Rectangular, rounded or square	10 (11.9) 15	10 (12.2) 15	5 (5.1) 7.5	Pointed	–	–	–	–	–	–	–
Pycreus tener	Rectangular or rounded	7.5 (12.3) 17.5	7.5 (12.5) 17.5	5	Pointed	Polygonal	Smooth	4–7	7.5 (18.9) 30	17.5 (28.3) 50	7.5	Rounded
Rhynchospora corymbosa	Rectangular, rounded or square	10 (13.5) 22.5	10 (18.2) 27.5	5 (7.5) 7.5	Pointed	Polygonal	Smooth	4–7	10 (22.1) 45	15 (44.8) 92.5	7.5 (9.8) 22.5	Rounded or truncated
Schoenoplectus californicus	Rectangular, rounded or square	5 (9) 12.5	7.5 (11.3) 17.5	5	Pointed	–	–	–	–	–	–	–

[A]Minimum (median) maximum.
[B]Min–max.

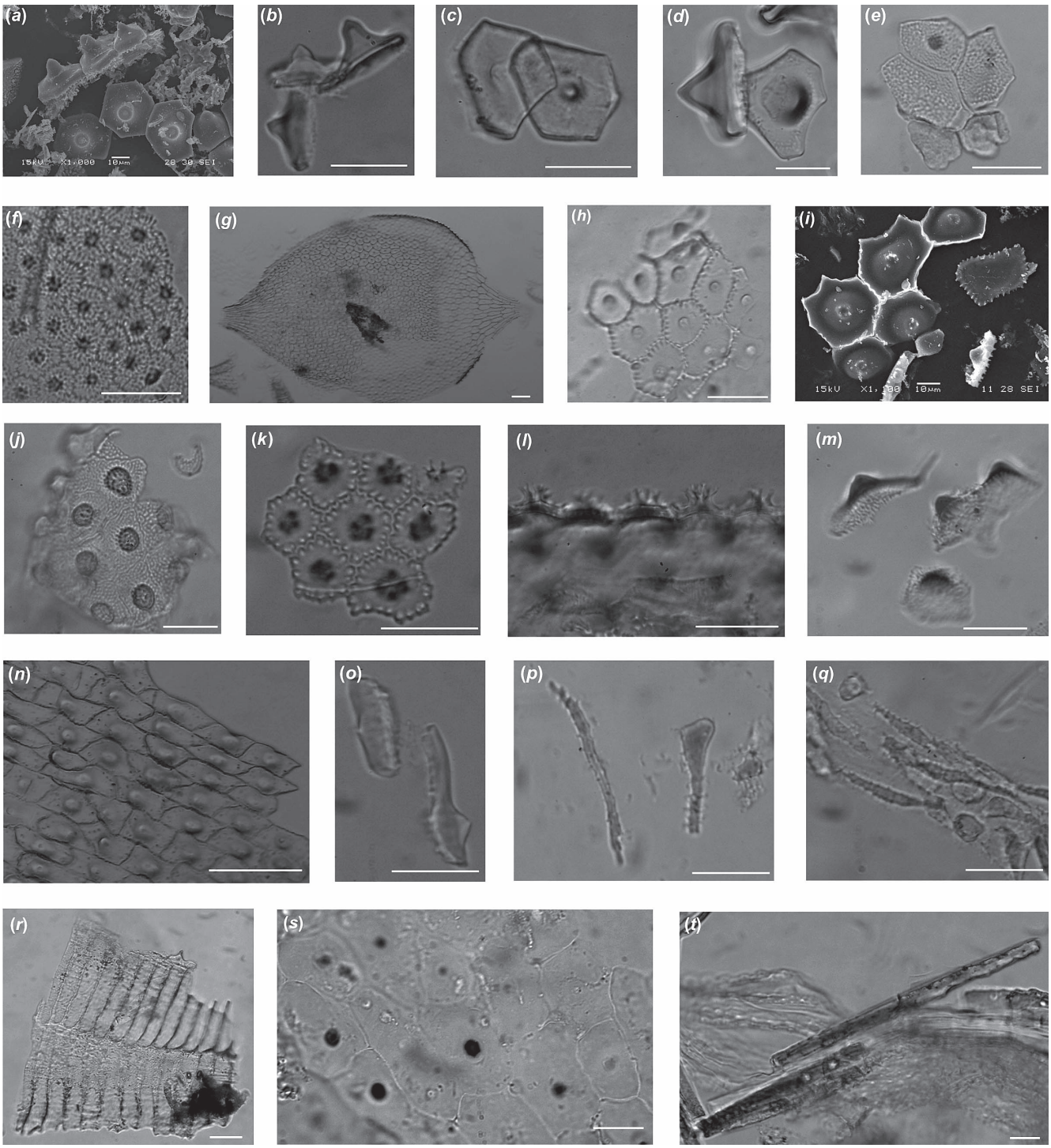

Fig. 4. Fruit assemblages. Polygonal cones in (*a*, *b*) *Carex chilensis*, (*c*) *Carex phalaroides*, (*d*) *Carex tweediana*, (*e*) *Cyperus corymbosus*, (*f*) *Cyperus digitatus*, (*g–i*) *Cyperus eragrostis*, (*j*) *Cyperus odoratus*, (*k*, *l*) *Cyperus reflexus*, (*m*) *Pycreus tener* and (*n*, *o*) *Rhynchospora corymbosa*. Cylindrical dendriform phytoliths in (*p*) *Carex tweediana* and (*q*)*Rhynchospora corymbosa*. (*r*) Silica skeletons (elongate phytoliths arranged in parallel rows) in *Eleocharis bonariensis*. (*s*) Polygonal base cones in *Schoenoplectus californicus*. (*t*) Elongate psilate in *Eleocharis macrostachya.* Scale bar = 25 µm for all, except for *g* = 50 µm, for *a*, *i* = 10 µm.

for Axis 2 and 12.10% for Axis 3) (Fig. 5*a*, *b*). Axes 1 and 2 showed the following four groups (Fig. 5*a*): Group I: *Eleocharis* spp. and *Schoenoplectus californicus*; Group II: *Pycreus tener*, *Cyperus odoratus*, *C. digitatus* and *C. corymbosus*; Group III: *C. reflexus*; and Group IV: *Carex* spp., *Rhynchospora corymbosa* and *Cyperus eragrostis*. Groups I and II were characterised by

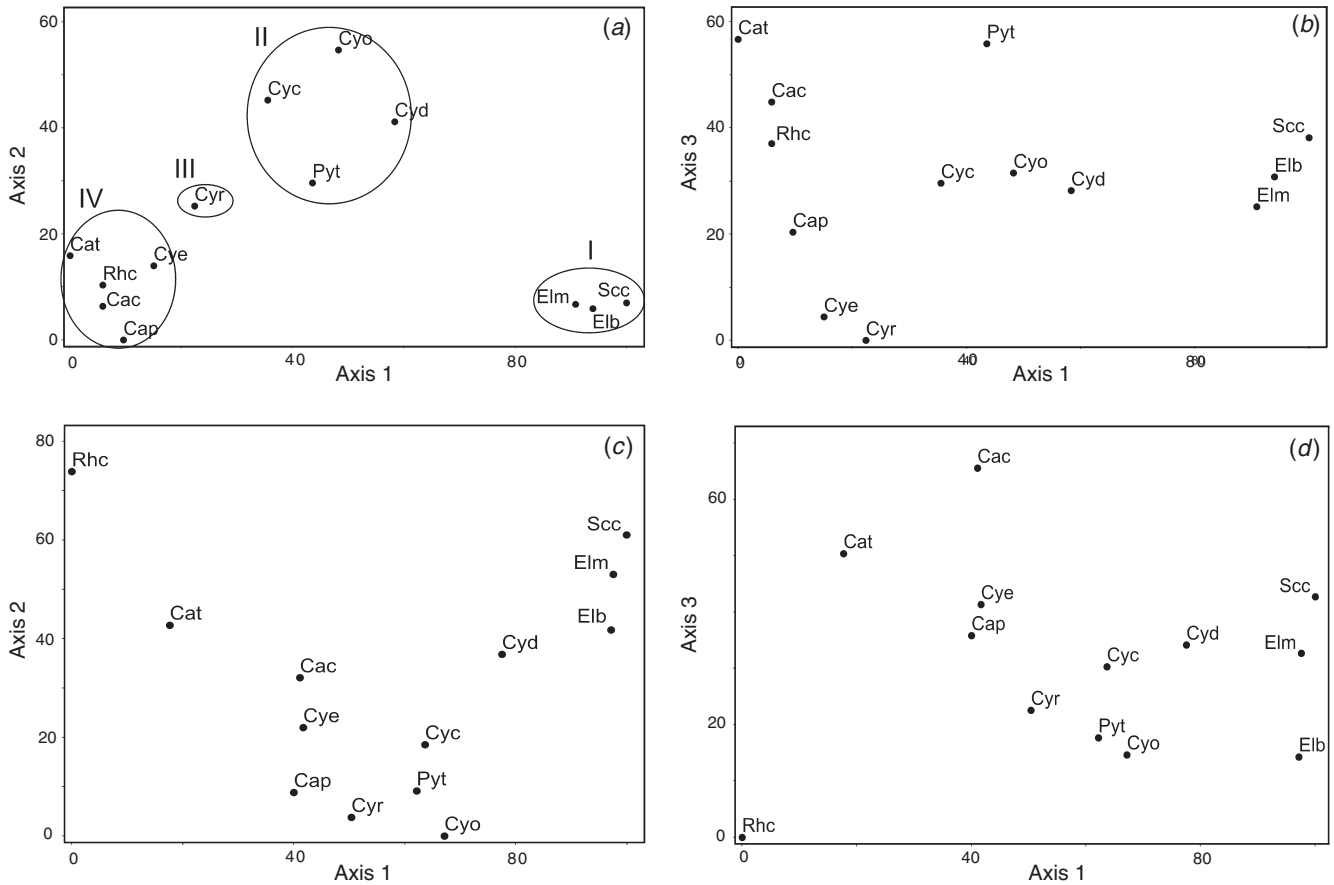

Fig. 5. PCA of species based on (*a*, *b*) qualitative and quantitative characters of cones and (*c*, *d*) cone characters and phytolith morphotypes. In (*a*) and (*c*) are represented Axes 1 and 2, and in (*b*) and (*d*) Axes 1 and 3. Groups I–IV are circled. Abbreviations of species are as given in Table 1.

cones with a smaller base and smaller apex; whereas Groups III and IV had bigger cones. Axis 3 separated species with the highest apex of the fruit cone (Fig. 5*b*). Figure 5*c*, *d* showed PCA based on the quantitative and qualitative characters of cone phytoliths and the relative frequencies of phytolith morphotypes. In this analysis, the three first axes accounted for 61.846% of the total variance. Some differences with the previous PCA were observed, as follows: *Rhynchospora corymbosa* was separated from *Carex* spp. and the *Cyperus eragrostis* group, and *Cyperus reflexus* was closer to *Cyperus* spp. and *Pycreus tener* group. In the first case, the abundance of stellate phytoliths in *R. corymbosa* could account for the separation from the group.

Discussion

The silica content of the leaves, culms and fruits analysed had a great variability not only within a genus, but also within a species. This pattern was mainly observed in *Cyperus* species, especially in the leaves of *C. reflexus*, and in the fruits of *Carex phalaroides*. The leaf values obtained were included in the range of values obtained by other researchers in the leaves of sedges (between 6 and 8%, Lanning and Eleuterius 1989) and in the leaves of other monocots as grasses (between 3 and 13%, Gallego *et al*. 2004; Fernández Honaine *et al.* 2008). Because of the variation found within species, silica content could not be considered as taxonomically useful. However, the quantification of silica in plants is relevant for other disciplines, such as biogeochemistry, and for studies of silica cycle (Conley 2002; Borrelli 2008; Borrelli *et al.* 2008). Quantification of the silica production should thus be included in phytolith analyses as an important aspect for the understanding of the silica cycle.

Although the most abundant phytolith morphotypes in leaf/culm and fruit assemblages are derived from epidermal cell silicifications (elongate, parallelepipedal, cones, stomatal complexes), the silicification process is also common in xylem (cylindrical sulcate tracheid phytoliths), parenchyma (stellate phytoliths) and sclerenchyma (cylindrical dendriform phytoliths) tissues. Stellate phytoliths (found in only one species, *Rhynchospora corymbosa*) are derived from the silicification of stellate cells of aerenchyma. This silica deposit was also observed by Gordon-Gray *et al.* (1978) and may be interpreted as a structural element that reinforces this common tissue. Cylindrical dendriform phytoliths may have been produced by the silicification of the lumen of certain sclerenchyma elements, such as brachysclereids, as suggested by Ragonese *et al.* (1984).

Conical phytoliths were the dominant morphotypes in all species studied, although there were differences between the cones in leaves/culms and those in fruit. These differences were mainly based on the shape of the base and on the dimensions of the whole cone. Leaf/culm cones had a rounded, rectangular

or square base shape; whereas typical fruit cones had a polygonal base and they were bigger and more robust. In many cases, leaf cones were also observed in fruit assemblages. These cones probably derived from glumes or utricles that were not discarded during the treatment. Toivonen and Timonen (1976) also found silica bodies in utricles from some *Carex* species that resemble the cones produced in leaves. *Eleocharis bonariensis*, *E. macrostachya* and *Schoenoplectus californicus* produced polygonal cones in very low quantities in their fruit assemblages. Considering that the selected material included some immature reproductive organs, and taking into account that other authors described these polygonal cones in *Schoenoplectus californicus* (Schuyler 1971), it is probable that these cones are produced once organ maturation is complete. Ragonese *et al.* (1984) found that the formation of silica bodies in two species of *Rhynchospora* is completed once achene is mature. The study of achenes of individuals of different maturity stages would corroborate this finding.

The results of the PCA based on quantitative and qualitative characters of cone phytoliths generally showed a separation among the genera studied here. This discrimination was improved by the incorporation of the relative frequencies of phytolith morphotypes. *Eleocharis* spp. and *Schoenoplectus californicus* grouping is probably a consequence of the lower percentage of polygonal cones in fruit assemblages and of the smaller size of the cones from culms. *Cyperus* spp. are related to *P. tener*, except for *C. eragrostis*, which is more closely associated with *Carex* spp. and *Rhynchospora corymbosa* group, probably owing to their similarity in cone size. In this last group, *R. corymbosa* is differentiated by the presence of stellate phytoliths. These results indicate that the incorporation of silica-body descriptions would be an important tool for understanding of taxonomic relationships among these genera, and among sedges in general (Toivonen and Timonen 1976; Menapace and Wujek 1987; Bruhl *et al*. 1992; Browning and Gordon-Gray 1995).

In summary, the paper presents the first detailed and comparative description of phytoliths and the first quantitative results of silica content in Argentine sedges. Some phytolith morphotypes, such as stellate phytoliths and cylindrical dendriform phytoliths, constitute the first description in this family. The morphological differences in cone production observed between organs could be a useful tool for palaeobotanical and/or archaeological studies, especially in those instances where phytoliths represent the only source of information of paleocommunities or human activities. Qualitative and quantitative characters of cone phytoliths, along with complete phytolith assemblages, allowed some distinction to be made among the genera studied. Finally, the present results represent the first step towards a construction of a detailed database of phytolith production of the Argentine sedges, essential for palaeoenvironmental, paleobotanical, archaeological, and also, taxonomical studies.

Acknowledgements

This work was supported by the Agencia Nacional de Promoción Científica y Tecnológica (PICT 1700, PICT 07 13864), Universidad Nacional de Mar del Plata (EXA 292/04) and CONICET (postgraduate fellowship to M. F. H.). We greatly thank Professor Rosa E. Guaglianone for the help in the identification and selection of the species, for the extensive bibliography and for the comments and suggestions on the first version of the manuscript, and Dr A. M. Avalos for the corrections and suggestions to the text.

References

Alexandre A, Meunier J, Lezine A, Vincens A, Schwartz D (1997) Phytoliths: indicators of grasslands dynamics during the late Holocene in intertropical Africa. *Palaeogeography, Palaeoclimatology, Palaeoecology* **136**, 213–229. doi: 10.1016/S0031-0182(97)00089-8

Barboni D, Bonnefille R, Alexandre A, Meunier JD (1999) Phytoliths as paleoenvironmental indicators, West Side Middle Awash Valley, Ethiopia. *Palaeogeography, Palaeoclimatology, Palaeoecology* **152**, 87–100. doi: 10.1016/S0031-0182(99)00045-0

Blinnikov MS (2005) Phytoliths in plants and soils of the interior Pacific Northwest, USA. *Review of Palaeobotany and Palynology* **135**, 71–98. doi: 10.1016/j.revpalbo.2005.02.006

Bonomo M, Zucol AF, Gutierrez Tellez B, Coradeghini A, Vigna MS (2009) Late Holocene palaeoenvironments of the Nutria Mansa 1 archaeological site, Argentina. *Journal of Paleolimnology* **41**, 273–296. doi: 10.1007/s10933-008-9225-3

Borba-Roschel M, Alexandre A, Varajão AFDC, Meunier JD, Varajão CAC, Colin F (2006) Phytoliths as indicators of pedogenesis and paleoenvironmental changes in the Brazilian *cerrado. Journal of Geochemical Exploration* **88**, 172–176. doi: 10.1016/j.gexplo.2005.08.032

Borrelli N (2008) Biomineralizaciones de sílice y calcio. Su rol en la biogeoquímica de Argiudoles típicos del sudeste bonaerense. PhD Thesis. Facultad de Ciencias Exactas y Naturales, Universidad Nacional de Mar del Plata, Argentina.

Borrelli N, Osterrieth M, Marcovecchio J (2008) Interrelations of vegetal cover, silicophytoliths content and pedogenesis of Typical Argiudolls of the Pampean Plain, Argentina. *Catena* **75**, 146–153. doi: 10.1016/j.catena.2008.05.001

Browning J, Gordon-Gray KD (1995) Studies in Cyperaceae in southern Africa 26: glume epidermal silica deposits as a character in generic delimitation of *Costularia* and *Cyathocoma* as distinct from *Tetraria* and other allies. *South African Journal of Botany* **61**, 66–71.

Bruhl JJ (1995) Sedge Genera of the world: relationships and a new classification of the Cyperaceae. *Australian Systematic Botany* **8**, 125–305. doi: 10.1071/SB9950125

Bruhl JJ, Watson L, Dallwitz MJ (1992) Genera of *Cyperaceae*: interactive identification and information retrieval. *Taxon* **41**, 225–234. doi: 10.2307/1222331

Chevalier A (2008) Early Holocene human adaptation in the Central Andes: what the phytoliths can tell us? In 'Interdisciplinary nuances in phytoliths and other microfossil studies'. (Eds MA Korstanje, MP Babot) pp. 149–160. (BAR International Series S1870: Oxford)

Conley DJ (2002) Terrestrial ecosystems and the global biogeochemical silica cycle. *Global Biogeochemical Cycles* **16**, 1121–1129. doi: 10.1029/2002GB001894

Duval-Jouve MJ (1873) Sur une forme de cellules épidermiques qui paraissent propres aux Cypéracées. *Bulletin Société Botanique de France* **20**, 91–95.

Fernández Honaine M, Zucol A, Osterrieth M (2006) Phytolith assemblage and systematic association in grassland species of the SE Pampean Plains, Argentina. *Annals of Botany* **98**, 1155–1165. doi: 10.1093/aob/mcl207

Fernández Honaine M, Bernava Laborde V, Zucol A (2008) Contenido de sílice en gramíneas del pastizal nativo del sudeste bonaerense. In 'Interdisciplinary nuances in phytoliths and other microfossil studies'. (Eds MA Korstanje, MP Babot) pp. 57–63. (BAR International Series S1870: Oxford)

Gallego L, Distel RA, Camina R, Rodriguez Iglesias RM (2004) Soil phytoliths as evidence for species replacement in grazed rangelands of Central Argentina. *Ecography* **27**, 725–732. doi: 10.1111/j.0906-7590.2005.03964.x

Gordon-Gray KD, van Laren L, Bandu V (1978) Silica deposits in *Rhynchospora* species (Cyperaceae). *Proceedings Electron Microscopy Society of Southern Africa* **8**, 83–84.

Iriarte J, Paz EA (2009) Phytolith analysis of selected native plants and modern soils from southeastern Uruguay and its implications for paleoenvironmental and archeological reconstruction. *Quaternary International* **193**, 99–123. doi: 10.1016/j.quaint.2007.10.008

Iriarte J (2006) Vegetation and climate change since 14,810 ^{14}C yr B.P. in southeastern Uruguay and implications for the rise of early Formative societies. *Quaternary Research* **65**, 20–32. doi: 10.1016/j.yqres.2005.05.005

Labouriau LG (1983) Phytolith work in Brazil: a minireview. *Phytolitharien Newsletter* **2**, 6–10.

Lanning FC, Eleuterius LN (1989) Silica deposition in some C_3 and C_4 species of grasses, sedges and composites in the USA. *Annals of Botany* **63**, 395–410.

Madella M, Alexandre A, Ball T (2005) International Code for Phytolith Nomenclature 1_0. *Annals of Botany* **96**, 253–260. doi: 10.1093/aob/mci172

Mehra PN, Sharma OP (1965) Epidermal silica cells in the Cyperaceae. *Botanical Gazette (Chicago, Ill.)* **126**, 53–58. doi: 10.1086/336295

Menapace FJ, Wujek DE (1987) The systematic significance of achene micromorphology in *Carex retrorsa* (Cyperaceae). *Brittonia* **39**, 278–283. doi: 10.2307/2807393

Metcalfe CR (1971) 'Anatomy of the monocotyledons. V. Cyperaceae.' (Clarendon Press: Oxford)

Ollendorf AL (1992) Toward a classification scheme of sedge (Cyperaceae) phytoliths. In 'Phytolith Systematics'. (Eds G Rapp, SC Mulholland) pp. 91–111. (Plenum Press: New York)

Piperno DR (1988) 'Phytolith analysis: an archaeological and geological perspective.' (Academic Press: San Diego, CA)

Ragonese AM, Guaglianone ER, Dizeo de Strittmatter C (1984) Desarrollo del pericarpio con cuerpos de sílice de dos especies de *Rhynchospora* Vahl. (Cyperaceae). *Darwiniana* **25**, 27–41.

Rovner I (1971) Potential of opal phytolith for use in paleoecological reconstruction. *Quaternary Research* **1**, 343–359. doi: 10.1016/0033-5894(71)90070-6

Schuyler AE (1971) Scanning electron microscopy of achene epidermis in species of *Scirpus* (Cyperaceae) and related genera. *Proceedings of the Academy of Natural Sciences of Philadelphia* **123**, 29–52.

Toivonen H, Timonen T (1976) Perigynium and achene epidermis in some species of *Carex*, subg. *Vignea* (Cyperaceae), studied by scanning electron microscopy. *Annales Botanici Fennici* **13**, 49–59.

Wilczek E (1892) Beiträge zur Kenntniss des Baues der Frucht und des Samens der Cyperaceen. *Botanisches Centralblatt* **51**, 129–138, 193–201.

Manuscript received 21 February 2009, accepted 20 August 2009